

Interfacial Rashba magnetoresistance of two-dimensional electron gas at LaAlO₃/SrTiO₃ interface

Kulothungasagaran Narayanapillai,^{1,*} Gyungchoon Go,^{2,*} Rajagopalan Ramaswamy,¹ Kalon Gopinadhan,¹ Dongwook Go,³ Hyun-Woo Lee,³ Thirumalai Venkatesan,^{1,4} Kyung-Jin Lee,^{2,5,†} and Hyunsoo Yang^{1,‡}

¹*Department of Electrical and Computer Engineering,
NUSNNI, National University of Singapore, 117576, Singapore*

²*Department of Materials Science and Engineering, Korea University, Seoul 02841, Korea*

³*PCTP and Department of Physics, Pohang University of Science and Technology, Pohang 37673, Korea*

⁴*Department of Physics, National University of Singapore, Singapore, 117542, Singapore*

⁵*KU-KIST Graduate School of Converging Science and Technology, Korea University, Seoul 02841, Korea*

(Dated: March 29, 2018)

We report the angular dependence of magnetoresistance in two-dimensional electron gas at LaAlO₃/SrTiO₃ interface. We find that this interfacial magnetoresistance exhibits a similar angular dependence to the spin Hall magnetoresistance observed in ferromagnet/heavy metal bilayers, which has been so far discussed in the framework of bulk spin Hall effect of heavy metal layer. The observed magnetoresistance is in qualitative agreement with theoretical model calculation including both Rashba spin-orbit coupling and exchange interaction. Our result suggests that magnetic interfaces subject to spin-orbit coupling can generate a nonnegligible contribution to the spin Hall magnetoresistance and the interfacial spin-orbit coupling effect is therefore key to the understanding of various spin-orbit-coupling-related phenomena in magnetic/non-magnetic bilayers.

PACS numbers: 85.75.-d; 73.20.-r; 75.47.-m; 75.70.Tj

I. INTRODUCTION

Recent advances in deposition techniques enable film growth control at the molecular level with atomic precision. These advances allow us to study exotic oxide materials with interesting properties. Since the discovery of two-dimensional electron gas (2DEG) formation at the interface of two insulating materials, LaAlO₃ (LAO) and SrTiO₃ (STO)¹, the LAO/STO system has emerged as one of the central material systems in the oxide community as it exhibits intriguing properties including superconductivity^{2,3} and ferromagnetism⁴⁻⁷. The ferromagnetism, which occurs on Ti site at the interface, has been evidenced by various measurement techniques such as scanning superconducting quantum interference device (SQUID)^{6,8}, X-ray magnetic circular dichroism⁷, torque magnetometry⁹, and magneto-transport¹⁰⁻¹⁶ driven by the Rashba spin-orbit coupling (SOC). Furthermore, the broken inversion symmetry at the interface results in the Rashba SOC which can be tuned by a gate voltage^{15,16}. Therefore, the LAO/STO interface is subject to both interfacial Rashba SOC and exchange coupling.

The magnetoresistance (MR) is a fundamental means to investigate charge and spin transport in condensed matter systems. In magnetic systems in the presence of SOC, the longitudinal resistance depends on the magnetization direction, e.g. anisotropic MR¹⁷. Recently, another type of angle-dependent MR, called spin Hall MR, was observed in ferromagnet (FM)/heavy metal (HM) bilayers¹⁸⁻²⁰. Including both anisotropic MR and spin Hall MR, the longitudinal resistivity is given as

$$\rho = \rho_0 + \Delta\rho_1 m_x^2 - \Delta\rho_2 m_y^2, \quad (1)$$

where ρ_0 is the magnetization-direction-independent re-

sistivity, $\Delta\rho_1$ ($\Delta\rho_2$) is the longitudinal resistivity change due to the anisotropic MR (spin Hall MR), and m_x (m_y) is the normalized magnetization component longitudinal (transverse) to the current-flow direction in the film plane. The original theory²¹ described the spin Hall MR as a consequence of bulk spin Hall effect (SHE) in HM by assuming no interfacial SOC effect. Recent theories however predicted an important role of the interfacial SOC at the FM/HM interface in the spin Hall MR^{22,23}.

Furthermore, several experiments on FM/HM bilayers suggested that the role of the interfacial SOC should be carefully examined. For example, it was reported for spin pumping and inverse SHE experiments on Co/Pt bilayers²⁴ that the total dissipated transverse spin current from Co layer (measured through the effective damping) is substantially different from the spin current absorbed in the bulk part of Pt layer (measured through inverse SHE). This difference was ascribed to the spin memory loss²⁵ describing the spin-flipping due to SOC at the Co/Pt interface²⁶. There were also spin-orbit torque experiments that cannot be explained by the bulk SHE mechanism alone but require an essential role of the interfacial SOC effect²⁷⁻³⁰. A recent experiment³¹ also found a close correlation, predicted for the interfacial SOC³², between the Dzyaloshinskii-Moriya interaction and field-like spin-orbit torque³².

Recent theories also suggested that the interfacial SOC effect is important for various SOC-related phenomena in FM/HM bilayers. First-principles approach^{33,34} showed that both SHE and inverse SHE are largely enhanced at the FM/HM interface, i.e., a manifestation of the interfacial SOC effect. Boltzmann transport calculations also suggested the importance of the interfacial SOC effect for various spin transport phenomena³⁵⁻³⁷.

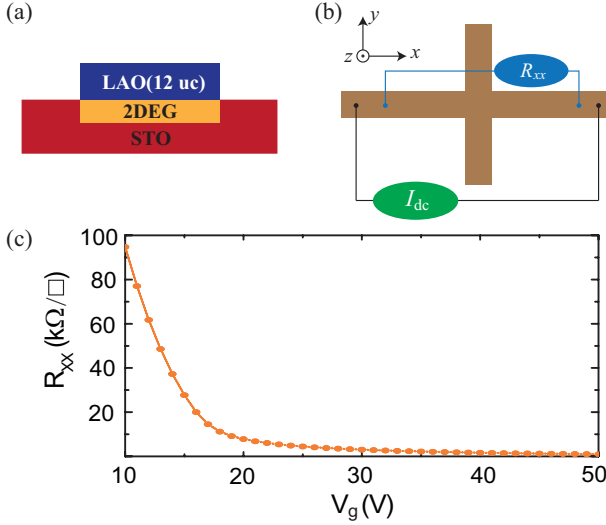


FIG. 1: (color online) (a) Schematics of LAO/STO stack layers, (b) Hall bar device with a measurement schematic for R_{xx} , and (c) The sheet resistance, R_{xx} , as a function of gate voltage V_g . At low gate voltages, the sample is insulating and the resistance monotonically decreases with increasing V_g .

Consequently, it is natural to raise a question about the role of the interfacial SOC in the spin Hall MR. Answering this question is of critical importance not only for understanding the underlying physics of SOC-related phenomena in FM/HM bilayers but also for enhancing the SOC effects for applications. For this purpose, we investigate the angular dependence of MR in 2DEG formed at the LAO/STO interface which has interfacial Rashba SOC and ferromagnetism. Unlike FM/HM bilayer structures where both bulk and interfacial SOC contributions coexist and it is therefore hard to differentiate one from the other, the LAO/STO 2DEG is an ideal system to investigate a pure interface effect because it is a single interface just like the FM/HM interface but does not have the bulk SHE.

II. EXPERIMENTS

The devices were prepared as follows. As shown in Fig. 1(a), LAO (12 unit cells; 1 u.c. = 0.379 nm) was grown on a TiO_2 terminated atomically smooth STO (001) single crystalline substrate, which was pre-treated with buffered oxide etch and air-annealed at 950 °C for 1.5 h, by pulsed laser deposition (PLD) at 750 °C in an oxygen partial pressure of 1 mTorr. The growth was monitored by in-situ reflective high energy electron diffraction. The sample was post-annealed at 750 °C in the presence of oxygen in order to remove oxygen vacancies. Electron beam lithography was utilized to define the Hall bar structure using a negative tone resist. A blanket AlN_x was deposited by PLD at room temperature followed by a lift-off process. Thereby, a 2DEG LAO/STO interface was

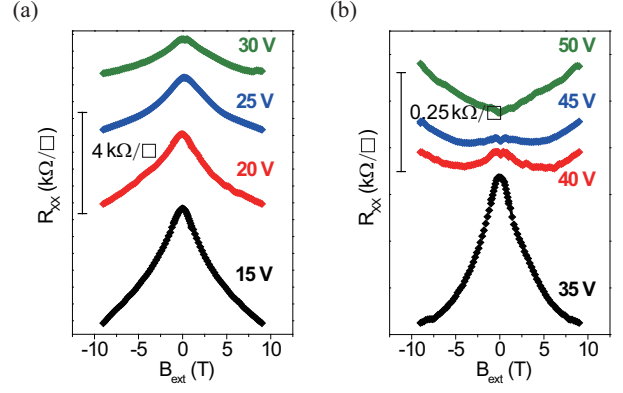


FIG. 2: (color online) Gate voltage dependence of R_{xx} . Perpendicular magnetic field dependence of R_{xx} for (a) $V_g = 15, 20, 25$ and 30 V, and (b) $V_g = 35, 40, 45$ and 50 V.

formed only at the defined device structure. The Hall bar channels were designed parallel to the sample edge to align the channels along the crystallographic axis (001).

A measurement scheme for longitudinal resistance (R_{xx}) is shown in Fig. 1(b). The electrical transport characterizations were performed in a physical property measurement system with a rotator used for angle-dependent MR measurements. We performed MR measurements as a function of various parameters including magnetic field B_{ext} , gate voltage V_g , and rotation plane of magnetic field. For the gating, a back gate voltage (V_g) was applied through STO as the dielectric and silver as the back gate contacts.

In Fig. 1(c), we depict a typical R_{xx} versus V_g curve at the temperature T of 2 K. We observe a monotonic decrease in R_{xx} with increasing V_g , showing that the device characteristic changes from insulating to conducting as V_g increases. Figure 2 shows the perpendicular magnetic field (B_{ext}) dependence of R_{xx} at various gate voltages. At low gate voltages ($V_g < 40$ V), R_{xx} decreases with increasing $|B_{\text{ext}}|$, which results from the weak localization (WL). At high gate voltages ($V_g > 45$ V), on the other hand, R_{xx} increases with increasing $|B_{\text{ext}}|$, which implies that the WL correction is sub-dominant in conducting regimes.

Figure 3 shows a representative result of the angle-dependent R_{xx} for three rotation angles of B_{ext} , i.e., α -rotation in the xy -plane, β -rotation in the yz -plane, and γ -rotation in the zx -plane (see Fig. 3 for the definition of the angles). Here the current is always applied in the x -direction. We observe that the normalized MR [$\equiv \tilde{R}_{xx} = (R_{xx}^{\text{max}} - R_{xx}^{\text{min}})/R_{xx}^{\text{min}}$] is about 7% in the α - and β -rotations, while it is about 3% in the γ -rotation³⁸. An important observation is that the angle-dependent change in \tilde{R}_{xx} is nonzero for the β -rotation. As the LAO/STO interface has no contribution from the bulk SHE, this noticeable change in \tilde{R}_{xx} for the β -rotation proves that $\Delta\rho_2$ term of Eq. (1) is nonzero for

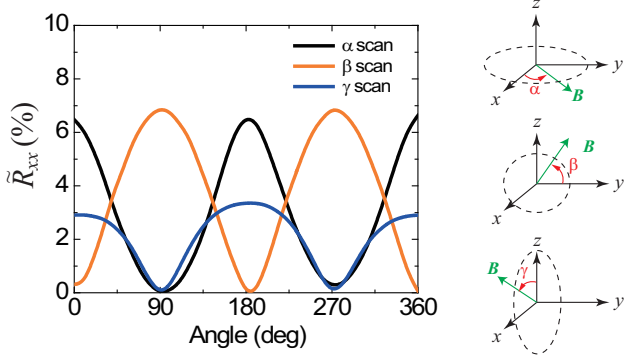


FIG. 3: (color online) Measured angular dependence of the normalized MR (\tilde{R}_{xx}) as a function of the rotating angle (α , β , and γ) with applied field of $B_{\text{ext}} = 9$ T and gate voltage $V_g = 45$ V.

the LAO/STO interface even without the bulk SHE. This angle-dependent MR at the LAO/STO interface can be named the interfacial Rashba MR as it originates from the Rashba SOC at the interface. Furthermore, it is noteworthy that the interfacial Rashba MR is much larger than the reported spin Hall MR of FM/HM structures (0.01–1%)^{18–20}.

We further measured the angular dependences of interfacial Rashba MR for the three rotations at various back gate voltages [Fig. 4(a)]. In the α (β)-rotation, the interfacial Rashba MR in general follows $\cos^2 \alpha$ ($-\cos^2 \beta$), consistent with Eq. (1). An exception appears for $V_g = 20$ V. At this gate voltage, R_{xx} in the α -rotation is asymmetric between 90 and 270 degrees. This asymmetry is attributed to a nonnegligible contribution from current-induced spin polarization as reported previously¹². For detailed description of the current-induced spin polarization to the magneto-resistive effect, see Ref. [39]. In the β -rotation, on the other hand, the sign of interfacial Rashba MR changes at $V_g = 20$ V. This sign change is attributed to the WL correction as the β -rotation involves the contribution of out-of-plane component of the magnetic field B_{ext} and the WL correction to R_{xx} becomes significant at low gate voltages (see Fig. 2).

III. THEORETICAL ANALYSIS

In order to understand the interfacial Rashba MR, we compute charge transport in the 2DEG at the LAO/STO interface. As an effective model which captures the qualitative features of the experimental results, we choose a simple model Hamiltonian \mathcal{H} as

$$\mathcal{H}(\mathbf{k}) = \frac{\hbar^2 \mathbf{k}^2}{2m} + \alpha_R \boldsymbol{\sigma} \cdot (\hat{\mathbf{z}} \times \mathbf{k}) + J \boldsymbol{\sigma} \cdot \hat{\mathbf{m}}, \quad (2)$$

where $\mathbf{k} [= (k_x, k_y)]$ is a two-dimensional wave vector, m is the effective mass of the d_{xy} band, \hbar is the reduced

Planck constant, α_R is the Rashba constant, J is the exchange coupling between the conduction electron spin $\boldsymbol{\sigma}$ (Pauli matrices) and unit localized magnetic moment $\hat{\mathbf{m}}$. Here we assume that the magnetization orientation ($\hat{\mathbf{m}}$) is aligned along the external magnetic field direction. In general, the Rashba constant depends on the magnetization orientation^{40,41}. In our model calculation, we ignore this angular dependence of the Rashba constant and show that qualitative features of the angle-dependent MR observed in experiment are described by a simple free electron model without considering additional angular dependence of physical properties. The choice of this Hamiltonian demands an explanation. Since the STO is a cubic perovskite, three t_{2g} orbitals are degenerate at the Γ point in the bulk STO. For STO-based interface, the d_{xy} band lies lower than the degenerate d_{yz} and d_{xz} bands due to the interface confinement^{42–44}. The 2DEG geometry leads to a circular Fermi surface for d_{xy} band and degenerate elliptical Fermi surfaces for d_{yz} and d_{xz} bands. In our experiment, the sample is conducting at high gate voltages and becomes insulating as the gate voltage decreases. Moreover, the α -rotation results of R_{xx} [Fig. 4(a)] show $\cos^2 \alpha$ -like dependence without the Lifshitz transition which was observed in Ref [10]. These results indicate that the Fermi level lies in the the lowest d_{xy} band and lowers as the gate voltage decreases. Therefore, in our theoretical analysis, we use a free-electron Hamiltonian with Rashba SOC and s - d exchange interaction by focusing on the single d_{xy} band. For simplicity, we treat the vector potential contribution to MR separately as the WL correction.

In our model calculation, we focus on the qualitative description of the longitudinal conductivity. In the high gate voltage regime where the WL correction is subdominant, the qualitative feature of the longitudinal conductivity is captured by the Kubo formula with the relaxation time approximation, given as

$$\sigma_{xx}^0 = 2e^2 \tau \sum_{n=\pm} \int \frac{d^2 k}{(2\pi)^2} (v_x^n)^2 \delta(E_n - E_F), \quad (3)$$

$$E_{\pm} = \frac{\hbar^2 \mathbf{k}^2}{2m} \pm |\alpha_R (\mathbf{k} \times \hat{\mathbf{z}}) + J \hat{\mathbf{m}}|, \quad (4)$$

$$v_x^{\pm} = \frac{\hbar k_x}{m} \pm \frac{\alpha_R}{\hbar} \left(\frac{J m_y + \alpha_R k_x}{|\alpha_R (\mathbf{k} \times \hat{\mathbf{z}}) + J \hat{\mathbf{m}}|} \right), \quad (5)$$

where $+/-$ represents spin up/down band, e is the electron charge, τ is the relaxation time, and E_F is the Fermi energy. In the experimental result depicted in Fig. 4(a), there are sign changes between low gate and high gate voltage regimes. In order to describe the electron transport in the low conductance (i.e., low gate) regime, we adopt the theoretical results of Ref. [45,46], which compute the WL correction as

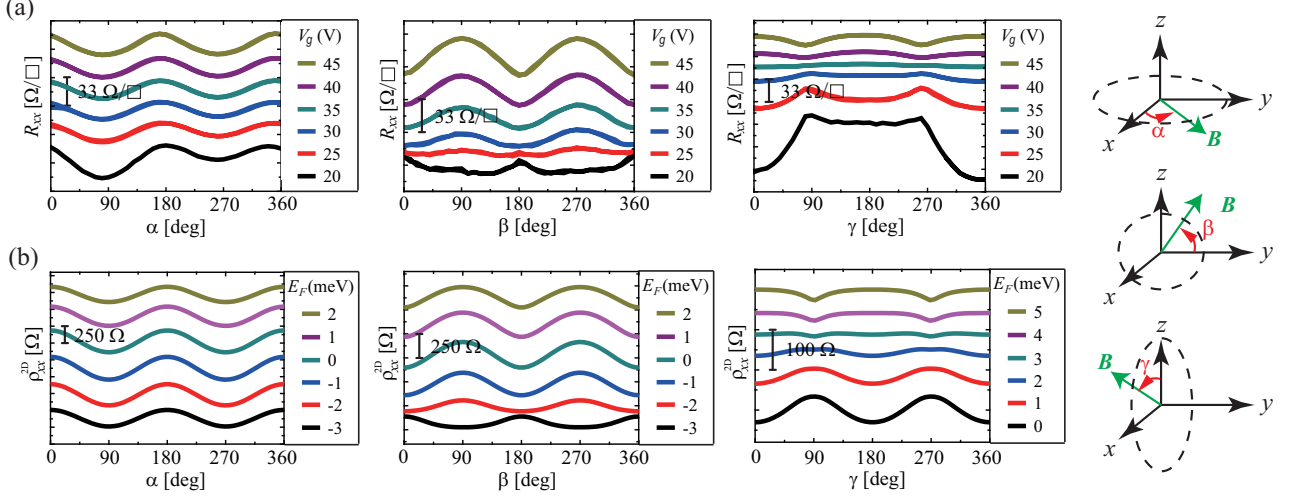


FIG. 4: (color online) (a) Experimental results of angular dependence of R_{xx} as a function of α -, β -, and γ -rotations with various V_g , and applied field $B_{\text{ext}} = 9$ T. (b) Theoretical calculations for angular dependence of the resistivity, ρ_{xx}^{2D} , as a function of α -, β -, and γ -rotations with various Fermi energies. The curves are offset along the y -axis for clarity.

$$\Delta\sigma_{xx}(B) = -\frac{e^2}{4\pi^2\hbar} \left\{ \frac{1}{a_0} + \frac{2a_0 + 1 + H_{SO}/B}{a_1[a_0 + H_{SO}/B] - 2H_{SO}/B} + 2\ln\frac{H_{tr}}{B} + \psi\left(\frac{1}{2} + \frac{H_\phi}{B}\right) + 3C \right. \\ \left. - \sum_{n=1}^{\infty} \left[\frac{3}{n} - \frac{3a_n^2 + 2a_n H_{SO}/B - 1 - 2(2n+1)H_{SO}/B}{[a_n + H_{SO}/B]a_{n-1}a_{n+1} - 2(H_{SO}/B)[(2n+1)a_n - 1]} \right] \right\}, \quad (6)$$

where $a_n = n + \frac{1}{2} + \frac{H_\phi}{B} + \frac{H_{SO}}{B}$, $\psi(1+z) = -C + \sum_{n=1}^{\infty} \frac{z}{n(n+z)}$ and C is the Euler constant. We note that Eq. (6) is a quantum correction to the conductivity due to a perpendicular magnetic field⁴⁷. We use the following parameters for the model calculations: $m = 0.7m_e$ (m_e is the free electron mass)¹⁶, $J = 2.5$ meV, $\tau = 0.33$ ps, $H_\phi = 3.0$ T, and $H_{SO} = 1.2$ T. For gate voltage effect on the Rashba coefficient, we assume $\alpha_R = (60 + \lambda E_F)$ meVÅ, where $\lambda = 4/\text{meV}$.

In Fig. 4(b), we show theoretical results for the angular dependence of the resistivity as functions of the rotating angles in α , β , and γ . The change in the gate voltage is considered as the change in the Fermi energy. The Fermi-energy shift for the γ -rotation is taken into account in order to reflect the resistance hysteresis from the voltage cycle³⁸. In all three rotations, the theoretical calculations of MR qualitatively matches well with the experimental results [Fig. 4(a)]. Even though our model Hamiltonian and calculation scheme is simplified, this good agreement shows that the simple Hamiltonian [Eq. (2)] considering the coexistence of Rashba SOC and exchange coupling describes the experimental result reasonably well and the interfacial Rashba SOC is key to the interfacial Rashba MR of which angular dependence is similar to that of the spin Hall MR.

In order to get an insight into the similarity between

the interfacial Rashba MR and the spin Hall MR, we focus on the second term in Eq. (5), which is an additional velocity originating from the Rashba interaction. This additional velocity includes the magnetization orientation that gives the angular dependence of the longitudinal conductivity. In other words, a strong m_y dependence of ΔR_{xx} is natural because of the symmetry of Rashba SOC. For instance, one obtains $v_x^\pm \approx \hbar k_x/m \pm Jm_y\alpha_R/\hbar$ for $J \gg \alpha k_F$. There is also an additional source of the angular dependence of the interfacial Rashba MR. When the Rashba SOC and exchange coupling coexist, the Fermi surface distorts depending on the magnetization direction⁵⁰. The Fermi surface distortion is maximized for an in-plane magnetization whereas it is absent for an out-of-plane magnetization. Because of these two contributions, additional velocity and Fermi surface distortion, the interface subject to both Rashba and exchange interactions exhibits the interfacial Rashba MR similar to the spin Hall MR.

IV. SUMMARY AND DISCUSSION

In summary, we report the interfacial Rashba MR for LAO/STO 2DEG and find that its angular dependence is similar to that of the spin Hall MR observed in FM/HM

structures. Our model calculations describe the experimental results reasonably and show that the spin-Hall-MR-like behavior originates from the combined effects of the interfacial Rashba SOC and exchange coupling. As the bulk spin Hall effect is absent in the LAO/STO 2DEG system, our finding evidences that the interfacial Rashba SOC gives rise to the spin-Hall-like MR. Therefore, our result suggests that the interfacial SOC effect is key to understanding of various SOC-related phenomena in magnetic/non-magnetic bilayers.

In the theory part of this work, we note that there are potential complexities left aside. In this paper, we use the free electron model of single orbital (d_{xy}) with the linear Rashba interaction. However, the LAO/STO 2DEG is composed of t_{2g} orbitals with nonquadratic energy dispersion and there is a report suggesting the existence of the cubic Rashba interaction⁵¹. Moreover, in our model, many parameters are difficult to be determined in experiment and a quantitative description including the quantum correction is not reliable. Thus, we restrict the purpose of model calculation to a qualitative description of the experimental observation.

We end this paper by noting that a recent experiment for a Bi/Ag/CoFeB metallic trilayer found the Rashba-Edelstein MR⁵², of which angular dependence is similar to that of the spin Hall MR. This Rashba-Edelstein MR originates from the combined action of two separate in-

terfaces, the Bi/Ag interface with Rashba SOC⁵³ and the Ag/CoFeB interface with the exchange splitting, through a spin diffusion process. In this trilayer including a conducting bulk, therefore, the charge-to-spin and spin-to-charge conversions at the Bi/Ag interface and the spin-dependent reflection at the Ag/CoFeB interface are separated. Because of this separation in the trilayer, it is not straightforward to get an insight into the bulk versus interface contributions to the spin Hall MR of the FM/HM bilayers. In contrast, our result gives a clear indication about the pure interface contribution to the spin Hall MR as the LAO/STO 2DEG, just like the FM/HM interface, is a single interface subject to both Rashba SOC and exchange coupling with no conducting bulk.

Acknowledgments

This work was supported by the National Research Foundation (NRF), Prime Ministers Office, Singapore, under its Competitive Research Programme (NRF CRP12-2013-01), the National Research Foundation of Korea (NRF-2015M3D1A1070465, NRF-2016R1A6A3A11935881, NRF-2017R1A2B2006119), and by the DGIST R&D Program of the Ministry of Science, ICT and Future Planning (17-BT-02).

* These two authors contributed equally to this work.

† Electronic address: kj_lee@korea.ac.kr

‡ Electronic address: eleyang@nus.edu.sg

¹ A. Ohtomo and H. Y. Hwang, *Nature* **427**, 423 (2004).

² N. Reyren *et al.*, *Science* **317**, 1196 (2007).

³ A. D. Caviglia, A. D. Caviglia, S. Gariglio, N. Reyren, D. Jaccard, T. Schneider, M. Gabay, S. Thiel, G. Hammerl, J. Mannhart, and J.-M. Triscone, *Nature* **456**, 624 (2008).

⁴ A. Brinkman, M. Huijben, M. Van Zalk, J. Huijben, U. Zeitler, J. C. Maan, W. G. Van Der Wiel, G. Rijnders, D. H. A. Blank, AND H. Hilgenkamp, *Nat. Mater.* **6**, 493 (2007).

⁵ Ariando, X. Wang, G. Baskaran, Z. Q. Liu, J. Huijben, J. B. Yi, A. Annadi, A. Roy Barman, A. Rusydi, S. Dhar, Y. P. Feng, J. Ding, H. Hilgenkamp, and T. Venkatesan, *Nat. Commun.* **2**, 188 (2011).

⁶ B. Kalisky, J. A. Bert, B. B. Klopfer, C. Bell, H. K. Sato, M. Hosoda, Y. Hikita, H. Y. Hwang, and K. A. Moler, *Nat. Commun.* **3**, 922 (2012).

⁷ J. S. Lee, Y. W. Xie, H. K. Sato, C. Bell, Y. Hikita, H. Y. Hwang, and C. C. Kao, *Nat. Mater.* **12**, 703 (2013).

⁸ J. A. Bert, B. Kalisky, C. Bell, M. Kim, Y. Hikita, H. Y. Hwang, and K. A. Moler, *Nat. Phys.* **7**, 767 (2011).

⁹ L. Li, C. Richter, J. Mannhart, and R. C. Ashoori, *Nat. Phys.* **7**, 762 (2011).

¹⁰ A. Joshua, J. Ruhman, S. Pecker, E. Altman, and S. Ilani, *Proc. Natl. Acad. Sci. USA* **110**, 9633 (2013).

¹¹ A. Annadi, Z. Huang, K. Gopinadhan, X. R. Wang, A. Srivastava, Z. Q. Liu, H. H. Ma, T. P. Sarkar, T. Venkatesan, and Ariando, *Phys. Rev. B* **87**, 201102 (2013).

¹² K. Narayanapillai, K. Gopinadhan, X. Qiu, A. Annadi, Ariando, T. Venkatesan, and H. Yang, *Appl. Phys. Lett.* **105**, 162405 (2014).

¹³ M. Diez, A. M. R. V. L. Monteiro, G. Mattoni, E. Cobanera, T. Hyart, E. Mulazimoglu, N. Bovenzi, C.W. J. Beenakker, A. D. Caviglia, *Phys. Rev. Lett.* **115**, 016803 (2015).

¹⁴ A. Fête, S. Gariglio, A. D. Caviglia, J.-M. Triscone, and M. Gabay, *Phys. Rev. B* **86**, 201105(R) (2012).

¹⁵ A. D. Caviglia, M. Gabay, S. Gariglio, N. Reyren, C. Cancellieri, and J. M. Triscone, *Phys. Rev. Lett.* **104**, 126803 (2010).

¹⁶ S. Hurand, A. Jouan, C. Feuillet-Palma, G. Singh, J. Biscaras, E. Lesne, N. Reyren, A. Barthelémy, M. Bibes, J. E. Villegas, C. Ulysse, X. Lafosse, M. Pannetier-Lecoeur, S. Caprara, M. Grilli, J. Lesueur, and N. Bergeal, *Sci. Rep.* **5**, 12751 (2015).

¹⁷ W. Thomson, *Proc. Royal Soc.* **8**, 546-550 (1857).

¹⁸ H. Nakayama, M. Althammer, Y.-T. Chen, K. Uchida, Y. Kajiwara, D. Kikuchi, T. Ohtani, S. Geprägs, M. Opel, S. Takahashi, R. Gross, G. E. W. Bauer, S. T. B. Goennenwein, and E. Saitoh, *Phys. Rev. Lett.* **110**, 206601 (2013).

¹⁹ S. Cho, S.-h.C. Baek, K.-D. Lee, Y. Jo, and B.-G. Park, *Sci. Rep.* **5**, 14668 (2015).

²⁰ J. Kim, P. Sheng, S. Takahashi, S. Mitani, and M. Hayashi, *Phys. Rev. Lett.* **116**, 097201 (2016).

²¹ Y.-T. Chen, S. Takahashi, H. Nakayama, M. Althammer, S. T. B. Goennenwein, E. Saitoh, and G. E. W. Bauer, *Phys. Rev. B* **87**, 144411 (2013).

²² V. L. Grigoryan, W. Guo, G. E. W. Bauer, and J. Xiao,

- Phys. Rev. B **90**, 161412 (2014).
- ²³ S. S.-L. Zhang, G. Vignale, and S. Zhang, Phys. Rev. B **92**, 024412 (2015).
 - ²⁴ J.-C. Rojas-Sánchez, N. Reyren, P. Laczkowski, W. Savero, J.-P. Attané, C. Deranlot, M. Jamet, J.-M. George, L. Vila, and H. Jaffrès, Phys. Rev. Lett. **112**, 106602 (2014).
 - ²⁵ H. Kurt, R. Loloee, K. Eid, W. P. Pratt Jr., and J. Bass, Appl. Phys. Lett. **81**, 4787 (2002).
 - ²⁶ H. Y. T. Nguyen, W. P. Pratt Jr., and J. Bass, J. Magn. Mater. **361**, 30 (2014).
 - ²⁷ X. Fan, H. Celik, J. Wu, C. Ni, K.-J. Lee, V. O. Lorenzm, and J. Q. Xiao, Nat. Commun. **5**, 3042 (2014).
 - ²⁸ H. Kurebayashi *et al.*, Nat. Nanotech. **9**, 211 (2014).
 - ²⁹ X. Qiu, K. Narayanapillai, Y. Wu, P. Deorani, D.-H. Yang, W.-S. Noh, J.-H. Park, K.-J. Lee, H.-W. Lee, and H. Yang, Nat. Nanotech. **10**, 333 (2015).
 - ³⁰ Y.-W. Oh, S.-h. C. Baek, Y. M. Kim, H. Y. Lee, K.-D. Lee, C.-G. Yang, E.-S. Park, K.-S. Lee, K.-W. Kim, G. Go, J.-R. Jeong, B.-C. Min, H.-W. Lee, K.-J. Lee, and B.-G. Park, Nat. Nanotech. **11**, 878 (2016).
 - ³¹ A. J. Berger, E. R. J. Edwards, H. T. Nembach, J. M. Shaw, A. D. Karenowska, M. Weiler, and T. J. Silva, arXiv:1611.05798.
 - ³² K.-W. Kim, H.-W. Lee, K.-J. Lee, and M. D. Stiles, Phys. Rev. Lett. **111**, 216601 (2013).
 - ³³ F. Freimuth, S. Blügel, and Y. Mokrousov, Phys. Rev. B **92**, 064415 (2015).
 - ³⁴ L. Wang, R. J. H. Wesselink, Y. Liu, Z. Yuan, K. Xia, and P. J. Kelly, Phys. Rev. Lett. **116**, 196602 (2016).
 - ³⁵ P. M. Haney, H.-W. Lee, K.-J. Lee, A. Manchon, and M. D. Stiles, Phys. Rev. B **87**, 174411 (2013).
 - ³⁶ V. P. Amin and M. D. Stiles, Phys. Rev. B **94**, 104419 (2016).
 - ³⁷ V. P. Amin and M. D. Stiles, Phys. Rev. B **94**, 104420 (2016).
 - ³⁸ We note that for the MR measurement, we sweep the field and gate voltage for a given angle-rotation. Because of the resistance hysteresis originating from the voltage cycle, the MR of an angle-rotation is not the same as the sum of MRs of other two angle-rotations.
 - ³⁹ S. D. Ganichev, M. Trushin, and J. Schliemann, arXiv:1606.02043 (2016).
 - ⁴⁰ M. Gmitra, A. Matos-Abiad, C. Draxl, and J. Fabian, Phys. Rev. Lett. **111**, 036603 (2013).
 - ⁴¹ L. Chen, M. Decker, M. Kronseder, R. Islinger, M. Gmitra, D. Schuh, D. Bougeard, J. Fabian, D. Weiss, and C.H. Back, Nat. Commun. **7**, 13802 (2016).
 - ⁴² Y. Kim, R. M. Lutchyn, and C. Nayak, Phys. Rev. B **87**, 245121 (2013).
 - ⁴³ Z. Zhong, A. Toth, and K. Held, Phys. Rev. B **87**, 161102 (2013).
 - ⁴⁴ G. Khalsa, B. Lee, and A. H. MacDonald, Phys. Rev. B **88**, 041302 (2013).
 - ⁴⁵ S. V. Iordanskii, Y. B. Lyanda-Geller, and G. E. Pikus, JETP Lett. **60**, 206 (1994).
 - ⁴⁶ W. Knap, C. Skierbiszewski, A. Zduniak, E. Litwin-Staszewska, D. Bertho, F. Kobbi, J. L. Robert, G. E. Pikus, F. G. Pikus, S. V. Iordanskii, V. Mosser, K. Zekentes, and Yu. B. Lyanda-Geller, Phys. Rev. B **53**, 3912 (1996).
 - ⁴⁷ For simplicity, we neglect the quantum correction from an in-plane magnetic field which is small compared to that from a perpendicular magnetic field at high field regimes (see Ref. [48,49]).
 - ⁴⁸ S. Maekawa and H. Fukuyama, J. Phys. Soc. Jpn. **50**, 2516 (1981).
 - ⁴⁹ F. Komori, S.-i. Kobayashi, Y. Ootuka, and W. Sasaki, J. Phys. Soc. Jpn. **50**, 1051 (1981).
 - ⁵⁰ K.-S. Lee, D. Go, A. Manchon, P. M. Haney, M. D. Stiles, H.-W. Lee, and K.-J. Lee, Phys. Rev. B **91**, 144401 (2015).
 - ⁵¹ H. Nakamura, T. Koga, and T. Kimura, Phys. Rev. Lett. **108**, 206601 (2012).
 - ⁵² H. Nakayama, Y. Kanno, H. An, T. Tashiro, S. Haku, A. Nomura, and K. Ando, Phys. Rev. Lett. **117**, 116602 (2016).
 - ⁵³ C. R. Ast, J. Henk, A. Ernst, L. Moreschini, M. C. Falub, D. Pacile, P. Bruno, K. Kern, and M. Grioni, Phys. Rev. Lett. **98**, 186807 (2007).